



Ground and excited state intramolecular proton transfer controlled intramolecular charge separation and recombination: A new type of charge and proton transfer reaction

Daobo Nie^a, Zuqiang Bian^{a,*}, Anchi Yu^b, Zhuqi Chen^a, Zhiwei Liu^a, Chunhui Huang^{a,*}

^a Beijing National Laboratory for Molecular Sciences, State Key Laboratory of Rare Earth Materials Chemistry and Applications, College of Chemistry and Molecular Engineering, Peking University, Beijing 100871, PR China

^b Department of Chemistry, Renmin University of China, Beijing 100872, PR China

ARTICLE INFO

Article history:

Received 9 November 2007

Accepted 27 February 2008

Available online 18 March 2008

Keywords:

Intramolecular proton transfer
Intramolecular charge transfer
Dual fluorescence

ABSTRACT

A novel β -diketone 1-(4-(9-carbazol)phenyl)-3-phenyl-1,3-propanedione (CDBM) has been synthesized. When excited at 380 nm, this molecule shows single fluorescence. However, when excited at 338 nm, it shows dual fluorescence. A Al^{3+} complex $\text{Al}(\text{CDBM})_3$ has been synthesized to investigate the dual fluorescence of CDBM. It is found that this complex shows single fluorescence under all excitation. This result indicated that the dual fluorescence of CDBM may relate to the intramolecular proton transfer reaction. Based on the experimental and theoretical studies of CDBM, *N*-(4-cyanophenyl)carbazole (CBN) and $\text{Al}(\text{CDBM})_3$, a “ground and excited state intramolecular proton transfer controlled intramolecular charge separation and recombination” mechanism is proposed to explain the unusual excitation-dependent dual fluorescence of CDBM.

© 2008 Elsevier B.V. All rights reserved.

1. Introduction

Charge and proton transfer reactions are both fundamental chemical processes occurring in nature. Intensive studies can be found in the literature for both subjects [1–6]. It is particularly interesting when both processes are feasible in one molecule. One prototype of such systems is 4'-(diethylamino)-3-hydroxyflavone [7,8]. This molecule exists in its energetically favorable normal form (N) in ground state. After excitation, it is promoted to the intramolecular charge transfer (ICT) excited state N^* . At the same time, N^* can be transformed into a tautomer form (T^*) through excited state intramolecular proton transfer (ESIPT) reaction. Dual fluorescence can be observed when the two forms decay to their corresponding ground states [7,8]. New cases have been reported such as HBOCE and HBODC, which show strong solvatochromic fluorescence from ESIPT/ICT process [4]. However, the dual fluorescence of these molecules is excitation-independent and the charge transfer (CT) is controlled by the intramolecular proton transfer only in the excited states.

In this paper, we report for the first time an interesting excitation-dependent dual fluorescence phenomenon of a donor–acceptor–acceptor type β -diketone 1-(4-(9-carbazol)phenyl)-3-phenyl-

1,3-propanedione (CDBM). This molecule shows single fluorescence (Band A), dual fluorescence (Bands A and B) as the excitation wavelength varies from 380 nm (around the first absorption band) to 338 nm (around the second absorption band). Both fluorescence bands show great solvatochromic shifts with increasing solvent polarity. In order to study the relationship between the dual fluorescence and the intramolecular hydrogen bonding of CDBM, the complex $\text{Al}(\text{CDBM})_3$ has been synthesized by coordinating CDBM to Al^{3+} ion. The photophysical properties (lifetimes and bathochromic shifts) of the model compound *N*-(4-cyanophenyl)carbazole (CBN), CDBM and $\text{Al}(\text{CDBM})_3$ have been studied systematically. The excited state dipole moments of the three compounds were determined with fluorescence solvatochromic method. Ground state geometries and energies of these compounds were calculated by density functional theory. Finally, the mechanism of the unusual excitation-dependent dual fluorescence of CDBM was discussed based on the experimental and theoretical investigations.

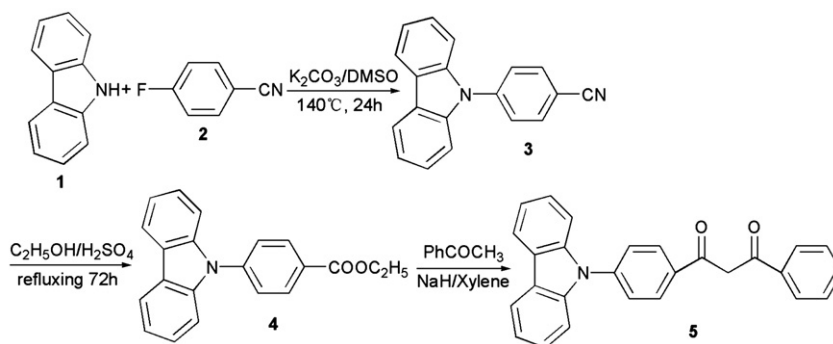
2. Experimental and computational details

2.1. Experimental details

N-(4-cyanophenyl)carbazole (CBN) was synthesized from 4-fluorobenzonitrile and carbazole by a simple procedure according to the literature [9]. The crude product was purified by

* Corresponding authors. Tel./fax: +86 10 62757156.

E-mail address: chhuang@pku.edu.cn (C. Huang).



Scheme 1. Synthetic procedure of CDBM.

recrystallization and subsequent column chromatography. CDBM was synthesized as follows (Scheme 1): 2.7 g (10 mmol) CBN, 15 ml H_2SO_4 and 50 ml $\text{C}_2\text{H}_5\text{OH}$ were added to a 100 ml round-bottomed flask and heated to reflux for 3 days. The mixture was poured into 500 ml water and then extracted with CH_2Cl_2 . The product ethyl 4-(9-carbazolyl)benzoate (**4** in Scheme 1) was purified by column chromatography with CH_2Cl_2 –petroleum ether (1:2, v/v) as eluent to give 2.41 g (76%) of **4**. To a three-neck flask (100 ml), sodium hydride (0.28 g, 70%, 16 mmol) washed with anhydrous hexane and anhydrous ether (60 ml), 2.41 g (8 mmol) **4** and 1.92 g (16 mmol) acetophenone were added sequentially. The mixture was stirred for 48 h under N_2 at room temperature and acidified by hydrochloric acid to pH 2–3, then the solvent was vaporized and the solid was purified by silica column chromatography with CH_2Cl_2 –petroleum ether (1:1, v/v) as eluent to give CDBM with yield of 42%. ^1H NMR (CD_3CN , TMS): δ (ppm) 7.16 (s, 1H), 7.33 (t, 2H, $J = 7.40, 7.04$ Hz), 7.46 (t, 2H, $J = 8.17, 7.21$ Hz), 7.51–7.59 (m, 4H), 7.65 (t, 1H, $J = 7.26, 7.27$ Hz), 7.79 (d, 2H, $J = 8.37$ Hz), 8.12 (d, 2H, $J = 7.36$ Hz), 8.20 (d, 2H, $J = 7.76$ Hz), 8.33 (d, 2H, $J = 8.43$ Hz), 17.14 (s, 1H). Anal. Calc. for $\text{C}_{27}\text{H}_{19}\text{NO}_2$: C, 83.27; H, 4.92; N, 3.60. Found: C, 83.08; H, 4.93; N, 3.44.

The complex $\text{Al}(\text{CDBM})_3$ was synthesized according to the following procedure: To a 50 ml round-bottomed flask, CDBM (1.167 g, 3.0 mmol), NaOH (0.120 g, 3.0 mmol) were mixed in 10 ml ethanol and refluxed for 10 min, then it was added dropwise to 10 ml ethanol solution of AlCl_3 (0.146 g, 1.1 mmol). The mixture was refluxed for 2 h and then poured into water. The crude product was obtained by filtration and purified by recrystallization in a mixture of THF–ethanol. ^1H NMR (CDCl_3 , TMS): δ (ppm) 7.11 (t, 3H, $J = 8.03, 7.56$ Hz), 7.29 (d, 6H, $J = 7.50$ Hz), 7.38–7.49 (m, 21H), 7.63–7.67 (m, 6H), 8.13 (t, 12H, $J = 8.12, 7.14$ Hz), 8.31–8.34 (m, 6H). Anal. Calc. for $\text{C}_{81}\text{H}_{54}\text{AlN}_3\text{O}_6$: C, 81.60; H, 4.57; N, 3.52. Found: C, 80.95; H, 4.72; N, 3.82.

All spectroscopic grade solvents were purchased from ACROS.

Absorption spectra were recorded with Shimadzu UV 3100 spectrophotometer, and steady state fluorescence spectra were taken with an Edinburgh Instruments FLS920 spectrometer. All the fluorescence spectra were corrected for the instrument response using a correction file provided by the manufactory. Fluorescence quantum yields were determined using quinine sulfate in 1.0 N H_2SO_4 as a standard ($\phi_f = 0.546$ at 25 °C) [10,11].

Lifetimes longer than 1 ns were measured with Edinburgh Instruments FLS920 based on the time correlated single photon counting technology. A hydrogen filled nanosecond flash lamp was used as the excitation source and the signals were detected with a photomultiplier (Hamamatsu R955). A picosecond lifetime spectrometer Edinburgh Instruments Lifespec-Red was used to measure lifetimes shorter than 1 ns. In this equipment, a diode laser (operating at 372 nm, pulse duration 69 ps) controlled by a picosecond light pulser (Hamamatsu PLP-10) was used as excita-

tion source. By processing the lifetime data with the F900 reconvolution software, a time resolution better than 1 ns for FLS920 and 20 ps for Lifespec-Red can be achieved.

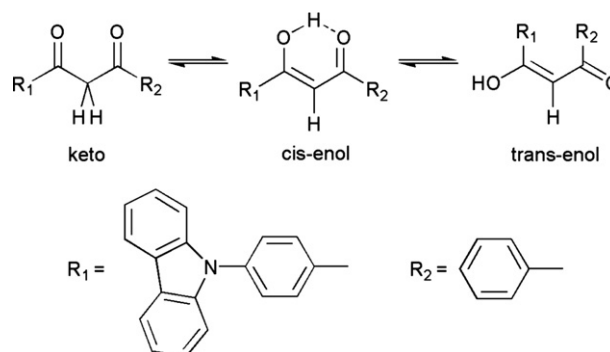
2.2. Computational details

The quantum chemical calculations were performed using the GAUSSIAN 03 package [12]. Ground state geometries of CBN, CDBM and $\text{Al}(\text{CDBM})_3$ have been optimized with the B3LYP [13] functional and a 6-31G(d) [14] basis set with no symmetry constraints. Numerical frequency calculations were performed with the same functional and basis set to determine the nature of the stationary point. The ground state dipole moments were calculated using the semi-empirical AM1 [15,16] method.

3. Results and discussion

3.1. Keto/enol equilibrium in solution

In general, β -diketones exist in three tautomeric forms in solution: keto, *cis*-enol and *trans*-enol form [17–19]. Scheme 2 illustrates the keto-enol equilibrium of CDBM. Because R_1 and R_2 are different, there are more than one *cis*-enol form and *trans*-enol form of CDBM. Scheme 2 only shows one of them for clarity. Among these tautomers, *cis*-enol forms are considered to be the photochemical stable ones because they are stabilized by the intramolecular hydrogen bonding and the conjugated system [17,20]. Theoretical studies have shown that the energies of *trans*-enol form β -diketones are much higher than their *cis*-enol isomers [20,21]. Therefore, they can only be observed experimentally at very low temperatures [21,22]. Because our experiments were all carried out at room temperature, it is reasonable to only consider the existence of keto and *cis*-enol forms. ^1H NMR spectrum of ca. 10^{-3} mol l^{-1} CDBM in



Scheme 2. Keto-enol equilibrium of CDBM.

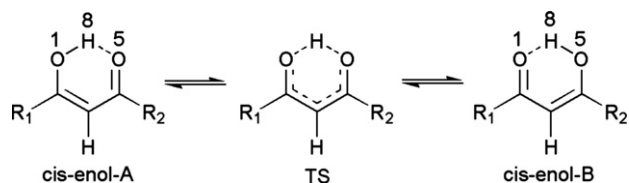
CD₃CN indicated that this molecule exists in solution predominantly as the *cis*-enol form (NMR signals at 17.0 ppm of OH and at 7.0 ppm of acetyl proton, no signal at 3.5–4.5 ppm corresponding to α -diketonic protons [23]). Based on the fact that the percentage of *cis*-enol forms will increase as the solvent polarity decreases [17], and that CH₃CN is the strongest polar solvent in our experiments, it is reasonable to suppose that CDBM exists mainly as the *cis*-enol forms in our experimental conditions. There are actually two possible structures of *cis*-enol form CDBM as shown in Scheme 3. In *cis*-enol-A, the intramolecular hydrogen bonding is O1–H8···O5 while in *cis*-enol-B, it is O5–H8···O1. These two *cis*-enol form isomers can transform into each other through a transition state (TS) [20]. Because the chemical environments of these two isomers are very similar to each other, it is possible that they are not distinguishable in the ¹H NMR spectrum. We calculated the relative energies of the two tautomers and the transition state (TS) with B3LYP/6-31G(d) method. The results showed that *cis*-enol-A (relaxed form) lies only 0.6 kJ mol⁻¹ above *cis*-enol-B (relaxed form) and the energy barrier between the two tautomers is about 9 kJ mol⁻¹. This energy difference between the two tautomers is so small that they should be able to exist in solution simultaneously.

3.2. Ground state structures

The B3LYP/6-31G(d) optimized 3D structures of the two *cis*-enol forms CDBM and Al(CDBM)₃ are illustrated in Fig. 1. The bond lengths of the central β -diketone fragment are also shown. As shown in Fig. 1, the DBM part (Chart 1) is nearly coplanar in all the three molecules. The carbazole moiety is twisted by about 50° with respect to phenyl ring I (Chart 1). The intramolecular hydrogen bonding of *cis*-enol-A is O1–H8···O5 and that of *cis*-enol-B is O5–H8···O1. Both intramolecular hydrogen bonds exhibit a bond length of 1.58 Å, which indicates strong hydrogen bonding in both isomers. In *cis*-enol-A form CDBM, C2–O1 is close to a single bond and C4–O5 is close to a double bond. However, the situation is totally opposite in *cis*-enol-B isomer. From this result we can infer that the Donor– π –Acceptor (D– π –A) system of *cis*-enol-B extends from the carbazole moiety through phenyl ring I to the carbonyl group C2–O1, while that of *cis*-enol-A spreads over the carbazole moiety, phenyl ring I, C2–C3, and carbonyl group C4–O5, which is obviously larger. Significant changes have taken place in the β -diketone part of CDBM after coordinating with Al³⁺. The intramolecular hydrogen bond has been eliminated and all the bond lengths in the β -diketone part (C–O bonds and C–C bonds) have been equalized. As a result, the β -diketone part loses its quinoid structure and exhibits a conjugated one. The whole β -diketone part can be regarded as the acceptor. Therefore, the D– π –A system of Al(CDBM)₃ should be extended from carbazole moiety through phenyl ring I to the center of β -diketone. Based on these facts, we suppose that the D– π –A system of Al(CDBM)₃ should be intermediate between those of *cis*-enol-A and *cis*-enol-B isomers.

3.3. Absorption

The absorption spectra of CBN, DBM, CDBM and Al(CDBM)₃ in CH₂Cl₂ are shown in Fig. 2. By comparing the absorption spectrum



Scheme 3. The equilibrium between the two *cis*-enol form CDBM. The structures of R₁ and R₂ are shown in Scheme 2.

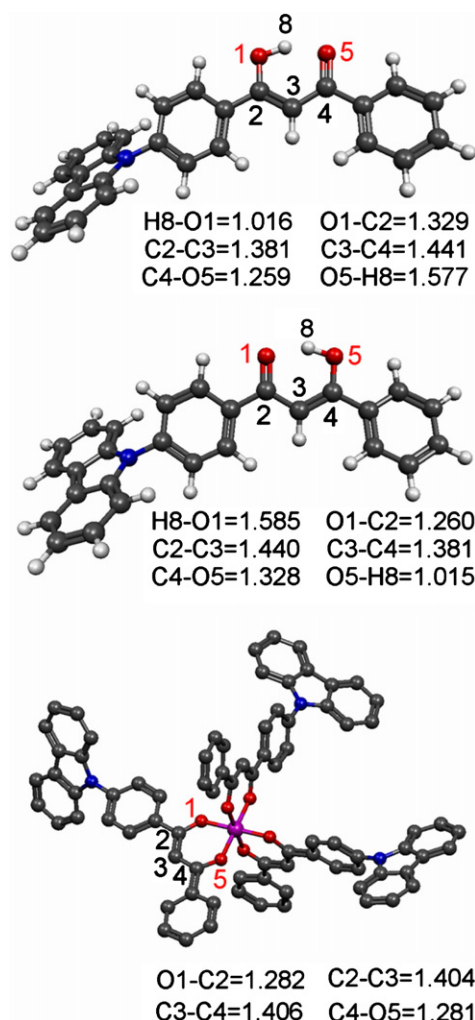


Fig. 1. The optimized structures of *cis*-enol-A (top), *cis*-enol-B (middle) and Al(CDBM)₃ (bottom). The bond lengths are in angstroms (Å). Hydrogen atoms in Al(CDBM)₃ are omitted for clarity.

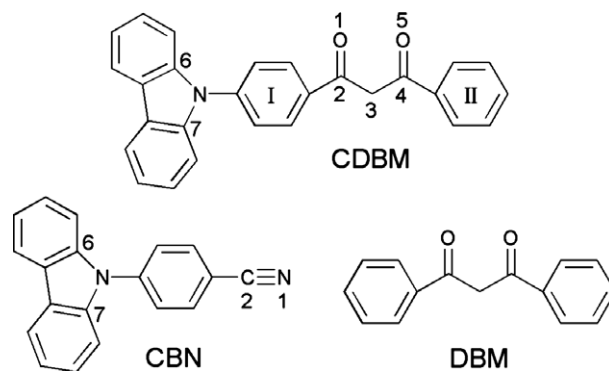


Chart 1. Molecular structure of CDBM, CBN and DBM.

of CDBM with that of DBM, it is reasonable to argue that the longest-wavelength absorption band (Ex 1 in Fig. 2, ~380 nm) and the shortest-wavelength band (~290 nm) is related to the carbazole moiety, which is the only difference between CDBM and DBM in molecular structure (Chart 1). The absorption spectra of CBN and CDBM are very similar from 260 nm to 338 nm. They both have a strong and structured absorption band around 290 nm. As

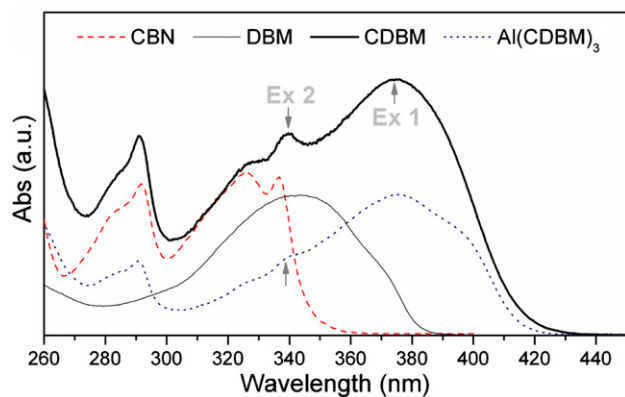


Fig. 2. Absorption spectra of CBN (dash), DBM (thin solid), CDBM (thick solid) and Al(CDBM)₃ (dot) in CH₂Cl₂.

carbazole showed a strong, sharp absorption band at 291.7 nm [24], we assigned this absorption band to the locally excited (LE) state ($\pi^* \leftarrow \pi$ transition) of the carbazole moiety. Around 338 nm, CDBM and CBN both show a sharp absorption band (Ex 2). Rettig and Zander assigned this band of CBN to a CT state which is populated by an electron transfer from carbazol moiety to the cyanophenyl part [25]. However, in the region above 350 nm, the absorption spectrum of CBN suddenly decreased to zero but CDBM showed a broad and strong absorption band around 380 nm. From Section 3.1 we know that there are two possible tautomers of CDBM in solution. Therefore, it is reasonable to suppose that the two absorption bands of CDBM (around 338 nm and 380 nm, respectively) may be related to the two tautomers (*cis-enol-A* and *cis-enol-B*).

3.4. Emission and excitation

CDBM exhibits interesting excitation-dependent dual fluorescence in solution. If the excitation varies from 350 nm to ~400 nm, CDBM will show single fluorescence (referred as “Band A”) in all solvents (Fig. 3, I). The spectrum shows vibrational structure in cyclohexane, suggesting partially LE character of the excited state [19]. In other solvents, the emission spectra show a broad structureless band which is strongly red-shifted as the solvent polarity increases. As the most characteristic phenomenon of charge transfer excited state is the bathochromic shift with increasing solvent polarity, this result indicates the CT character of Band A. However, if the excitation wavelength is shorter than 350 nm, CDBM will exhibit dual fluorescence in all solvents (Fig. 3, II). In addition to Band A, a new band (Band B) emerges on the short-wavelength side. This new band also shows a bathochromic shift with increasing solvent polarity, but not as prominent as Band A. In low polar solvents, Band B prevails. The intensity ratio of (Band B)/(Band A) gradually decreases as the solvent polarity increases. In strong polar solvents, Band A becomes dominate.

Because the fluorescence spectra depend on the excitation wavelength, it is important to investigate the excitation spectra of both emission bands. Fig. 4 shows the excitation spectra of CDBM monitored at both fluorescence bands together with the absorption spectra of CDBM and CBN in THF. As can be seen from Fig. 4, the excitation spectra monitored at both emission bands are quite different from each other, indicating different species in ground state. The one monitored at Band A is very similar to its absorption spectrum. However, the excitation spectrum monitored at Band B is quite different: in the region above 338 nm, it falls steeply down to zero. Interestingly, it closely resembles the

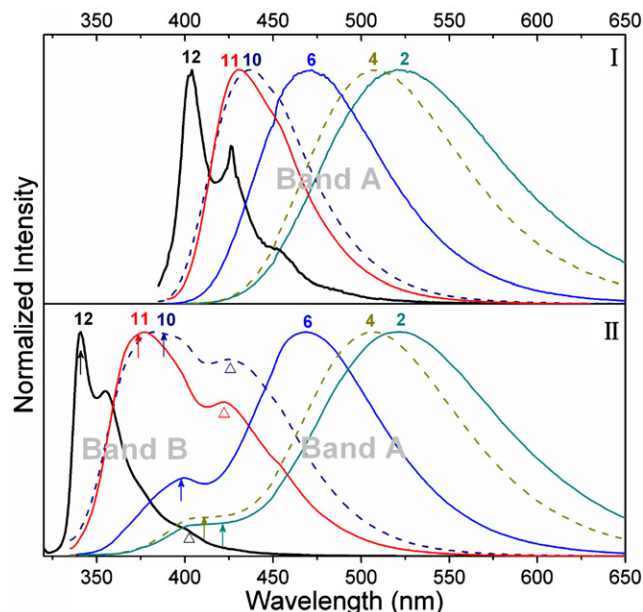


Fig. 3. Corrected fluorescence spectra of 1×10^{-5} M CDBM in various solvents. I: excited at 380 nm; II: excited at 330 nm. The numbers refer to solvents in Table 1. The arrows indicate the positions of Band B and the triangles denote the peaks of Band A. Please notice that arrows and triangles point to traces in the same color. (For interpretation of the references to colour in this figure legend, the reader is referred to the web version of this article.)

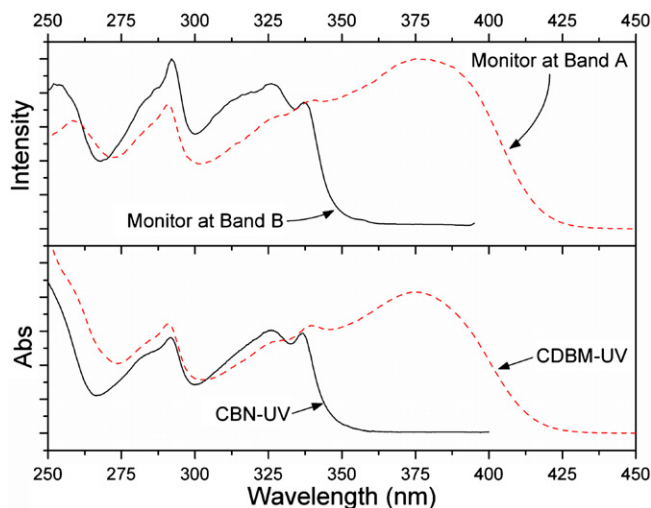


Fig. 4. Top panel: excitation spectra of 1×10^{-5} M CDBM in THF monitored at different emission bands. Bottom panel: UV-Vis spectra of 1×10^{-5} M CDBM and CBN in THF.

absorption spectrum of CBN. This result indicates that the molecular structure of the species corresponding to Band B may be similar to CBN.

As discussed in Section 3.1, *cis-enol-A* and *cis-enol-B* may both exist in solution. The excitation spectra monitored at both emission bands also indicate different species in ground state. Therefore, the excitation-dependent dual fluorescence may come from the two *cis-enol* forms of CDBM. To verify this assumption, we studied the fluorescence spectra of Al(CDBM)₃, in which the intramolecular hydrogen bonding of CDBM has been eliminated by coordinating with Al³⁺. The fluorescence spectra of Al(CDBM)₃ in THF under different excitation are shown in Fig. 5. The dual fluorescence spectrum of CDBM in THF is also depicted for comparison.

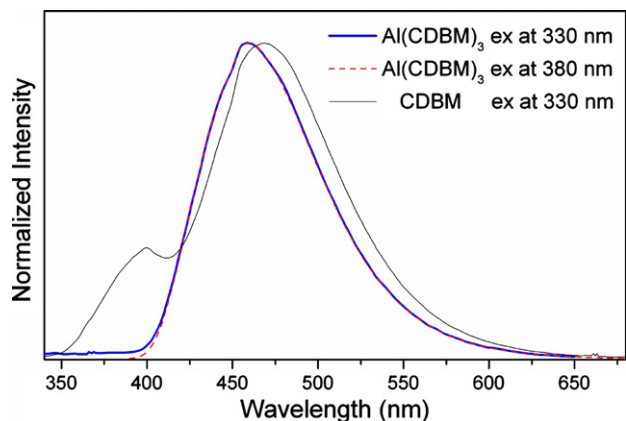


Fig. 5. The fluorescence spectra of Al(CDBM)₃ and CDBM in THF. Thick solid blue line: Al(CDBM)₃ excited at 330 nm; dashed red line: Al(CDBM)₃ excited at 380 nm; thin solid black line: CDBM excited at 330 nm. (For interpretation of the references to colour in this figure legend, the reader is referred to the web version of this article.)

As expected, Al(CDBM)₃ showed single fluorescence independent of the excitation wavelength. This result strongly suggests that the dual fluorescence of CDBM is caused by the intramolecular proton transfer reaction, which results in the equilibrium between *cis*-enol-A and *cis*-enol-B.

However, the corresponding relationship between the two emission bands and the two tautomers is still unclear. In order to solve this problem, we studied the photophysical properties (band positions and lifetimes) of CBN, *cis*-enol-A, *cis*-enol-B and Al(CDBM)₃ in various solvents. The results are listed in Table 1. It can be noticed from Table 1 that all the emission bands showed strong bathochromic shifts with increasing solvent polarity, indicating charge transfer nature of their corresponding excited states. The lifetimes of the four species are all in a nanosecond range (except for Band A in cyclohexane) which is two or three orders of magnitude longer than the solvent orientational times. Based on this fact, the relaxed excited state dipole moments can be estimated employing the modified Lippert–Mataga equation (1) [17,26–31]:

$$h\tilde{\nu}_{\text{flu}}^{\text{CT}} \cong h\tilde{\nu}_{\text{flu}}^{\text{vac}} - \frac{2\bar{\mu}_e(\bar{\mu}_e - \bar{\mu}_g)}{4\pi\epsilon_0 a_0^3} \left[\frac{\epsilon - 1}{2\epsilon + 1} - \frac{1}{2} \frac{n^2 - 1}{2n^2 + 1} \right] \quad (1)$$

where h is the Planck constant, c is the speed of light in vacuum, $\tilde{\nu}_{\text{flu}}^{\text{CT}}$ and $\tilde{\nu}_{\text{flu}}^{\text{vac}}$ are the CT fluorescence band positions in solution and in vacuum, respectively, $\bar{\mu}_g$ and $\bar{\mu}_e$ are the dipole moments of the sol-

ute in the ground and excited states, respectively, ϵ_0 is the absolute permittivity of vacuum, a_0 is the effective radius of the Onsager cavity [26], ϵ is the static dielectric constant, and n is the refractive index of the solvent. By plotting $\tilde{\nu}_{\text{flu}}^{\text{CT}}$ against the solvent polarity parameter $f(\epsilon, n) = [f(\epsilon) - 0.5f(n)]$, where

$$f(\epsilon) = \frac{\epsilon - 1}{2\epsilon + 1}; \quad f(n) = \frac{n^2 - 1}{2n^2 + 1} \quad (2)$$

we can get the values of $2\bar{\mu}_e(\bar{\mu}_e - \bar{\mu}_g)/4\pi\epsilon_0 a_0^3$. To determine the excited state dipole moment, we need to know the ground state dipole moment μ_g , the radius of the Onsager cavity a_0 and the angle between μ_e and μ_g . We performed AM1 calculations on the B3LYP/6-31G(d) optimized structures of CBN, *cis*-enol-A, *cis*-enol-B CDBM and Al(CDBM)₃ and got ground state dipole moments 2.52 D, 2.54 D, 3.00 D, 2.09 D for the four structures, respectively. As all the ground state dipole moments are very small, we ignored the angle between μ_e and μ_g . The estimation of a_0 is very important to determine μ_e as it enters the equation to the third power. Different authors have taken different approaches to calculate the value of a_0 [32–34]. We used the procedure recommended by Karpiuk in a recent paper [32]. For CBN, we estimated a_0 to be half the average distance of C6–N1 (see Chart 1 for atom numbering) and C7–N1 and got $a_0 = 3.86$ Å. For *cis*-enol-B form CDBM (Band B), half the average distance of C6–O1 and C7–O1 was taken and we got $a_0 = 3.64$ Å. For *cis*-enol-A form CDBM (Band A), we took half the average distance of C6–O5 and C7–O5 and yielded $a_0 = 4.70$ Å. In Al(CDBM)₃, the two oxygen atoms (O1 and O5) both act as the acceptor groups, so we took the average a_0 of the two *cis*-enol forms and got 4.17 Å. With all these results and the data in Table 1, we obtained the excited state dipole moments and the results are listed in Table 2. Samanta employed a “time-resolved microwave dielectric loss” method to determine the excited state dipole moment of CBN to be 10.4 D [35], which is very close to our result (10.1 D). This agreement proved our method to be reliable. It can be seen from Table 2 that the excited state dipole moment of Band B is very close to that of CBN. However, Band A shows a much larger excited state dipole moment. From Section 3.2 we know that the D– π –A system of

Table 2

Ground and excited state dipole moments of CBN, *cis*-enol-B, *cis*-enol-A and Al(CDBM)₃

Molecule	μ_g (D)	a_0	Fluorescence slope (cm ⁻¹)	μ_e (D)
Al(CDBM) ₃	2.09	4.17	–18111	12.4
Band A	2.54	4.70	–20246	15.7
Band B	3.00	3.64	–14923	10.0
CBN	2.52	3.86	–13670	10.1

Table 1

CT emission band positions (cm⁻¹, nm in the parentheses) and lifetimes (ns) for Al(CDBM)₃, CDBM and CBN in various solvents

Solvent	$f(\epsilon, n)^a$	Al(CDBM) ₃		Band A		Band B		CBN	
		Peak	τ (ns)	Peak	τ (ns)	Peak	τ (ns)	Peak	τ (ns)
Acetonitrile (1)	0.393	18,250 (548)	4.8	17,890 (559)	3.9	22,990 (435)	7.9	23,810 (420)	7.5
Acetone (2)	0.374	19,720 (507)	4.1	19,190 (521)	5.2	23,700 (422)	6.7	24,810 (403)	6.6
1,2-Dichloroethane (3)	0.326	19,920 (502)	4.7	19,650 (509)	5.8	24,210 (413)	8.3	24,940 (401)	7.6
Dichloromethane (4)	0.319	20,330 (492)	3.6	19,650 (509)	5.5	23,980 (417)	7.9	24,940 (401)	7.4
Methyl acetate (5)	0.308	20,620 (485)	2.2	19,530 (512)	3.2	24,690 (405)	7.0	25,060 (399)	6.3
THF (6)	0.307	21,690 (461)	1.0	21,230 (471)	2.0	25,130 (398)	6.0	25,450 (393)	5.8
Ethyl acetate (7)	0.292	21,500 (465)	1.2	21,370 (468)	2.1	25,060 (399)	5.6	25,450 (393)	5.2
<i>n</i> -Butyl acetate (8)	0.266	22,170 (451)	0.6	21,830 (458)	1.2	25,320 (395)	5.7	25,710 (389)	5.0
Trichloromethane (9)	0.256	21,930 (456)	0.9	20,700 (483)	3.2	24,330 (411)	6.5	25,190 (397)	5.9
Aether (10)	0.253	23,040 (434)	0.2	22,830 (438)	0.2	25,770 (388)	4.1	26,530 (377)	3.8
Toluene (11)	0.126	23,260 (430)	0.4	23,260 (430)	0.1	26,530 (377)	4.1	26,740 (374)	4.0
Cyclohexane (12)	0.100	24,390 (410)	0.1	24,810 (403) ^b	<0.02	28,990 (345)	3.6	28,990 (345)	3.5

^a Solvent polarity parameter, see Eq. (2) in the following text.

^b The emission band position corresponding to 0–0 transition.

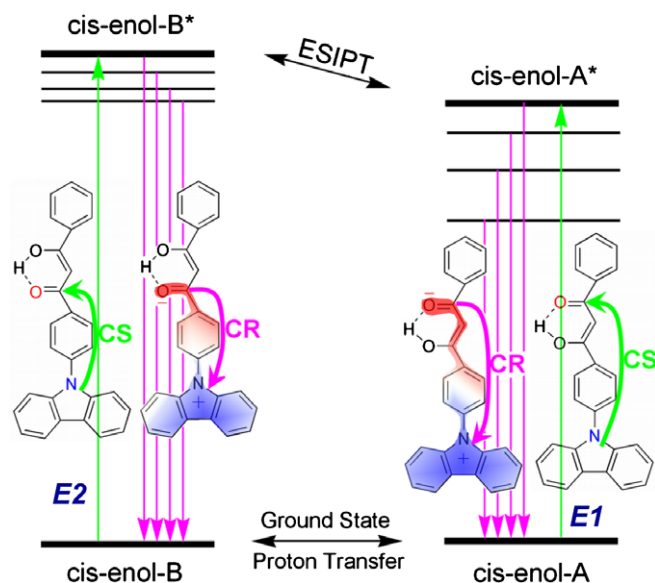


Fig. 6. Schematic representation of the excitation-dependent dual fluorescence mechanism of CDBM. CS: charge separation; CR: charge recombination.

cis-enol-B is very close to that of CBN, while that of *cis-enol-A* is obviously larger. Larger D- π -A system usually results in larger excited state dipole moment. Therefore, we concluded that Band A and Band B originate from *cis-enol-A* and *cis-enol-B*, respectively. The excited state dipole moment of Al(CDBM)₃ is smaller than *cis-enol-A* larger than *cis-enol-B*. This is because the D- π -A system of Al(CDBM)₃ is intermediate between *cis-enol-A* and *cis-enol-B* due to the coordination effect.

3.5. Excitation-dependent dual fluorescence of CDBM

Based on the results and discussions presented above, a possible mechanism of the excitation-dependent dual fluorescence of CDBM is illustrated in Fig. 6. In ground state, the two tautomers are very close in energy and can exist in solution simultaneously. The ground state intramolecular proton transfer reaction controlled the equilibrium between the two tautomers and further modulated the charge separation direction during excitation (see the green arrows in Fig. 6). Because the excited state dipole moment of *cis-enol-A* is larger than that of *cis-enol-B*, the excited state energy of the former should be lower than the latter due to solvent stabilization. Thus, low-energy excitation ($E_2 > E_1$) can only generate *cis-enol-A**. In this case, ESIPT would not happen because extra energy is needed to overcome the energy barrier from *cis-enol-A** to *cis-enol-B**. As a result, only single fluorescence corresponding to *cis-enol-A** is observed. If the excitation energy exceeds a certain threshold ($E_2 > E_1$), both tautomers can be promoted to their corresponding excited states; moreover, there is enough extra energy for the two tautomers to transform into each other through ESIPT. Dual fluorescence appears when both species relax to their corresponding ground states. During the period after excitation and before emission, ESIPT actually controlled the charge recombination direction (see the pink arrows in Fig. 6). As the solvent polarity increases, *cis-enol-A** will be stabilized by solvation more prominently than *cis-enol-B** due to its larger dipole moment. As a result, the equilibrium will shift to the *cis-enol-A** side and Band A will become dominant.

4. Conclusion

We report a novel synthesized β -diketone CDBM which displays a new type of charge and proton transfer reaction. Based on the

experimental and theoretical studies, it is concluded that the unusual excitation-dependent dual fluorescence originates from the charge transfer reaction which is controlled by the intramolecular proton transfer reaction in both ground and excited states.

Acknowledgement

The authors thank the National Basic Research Program (G2006CB601103), National Nature Science Foundation of China (20471004, 20490210, 20021101, 90401028) for financial support.

Appendix A. Supplementary data

Cartesian coordinates for the optimized geometries of *cis-enol-A*, *cis-enol-B* form CDBM and Al(CDBM)₃. Supplementary data associated with this article can be found, in the online version, at doi:10.1016/j.chemphys.2008.02.065.

References

- [1] Z.R. Grabowski, K. Rotkiewicz, W. Rettig, Chem. Rev. 103 (2003) 3899.
- [2] G.J. Woolfe, P.J. Thistlethwaite, J. Am. Chem. Soc. 103 (1981) 6916.
- [3] A.J.G. Strandjord, S.H. Courtney, D.M. Friedrich, P.F. Barbara, J. Phys. Chem. 87 (1983) 1125.
- [4] J. Seo, S. Kim, S.Y. Park, J. Am. Chem. Soc. 126 (2004) 11154.
- [5] A.S. Klymchenko, V.G. Pivovarenko, A.P. Demchenko, J. Phys. Chem. A 107 (2003) 4211.
- [6] R.V. Pereira, M.H. Gehlen, J. Phys. Chem. A 110 (2006) 7539.
- [7] T.C. Swinney, D.F. Kelley, J. Chem. Phys. 99 (1993) 211.
- [8] P.T. Chou, M.L. Martinez, J.H. Clements, J. Phys. Chem. 97 (1993) 2618.
- [9] R.F. Bridger, D.A. Law, D.F. Bowman, B.S. Middleton, K.U. Ingold, J. Org. Chem. 33 (1968) 4329.
- [10] W.H. Melhuish, J. Phys. Chem. 65 (1961) 229.
- [11] G.A. Crosby, J.N. Demas, J. Phys. Chem. 75 (1971) 991.
- [12] M.J. Frisch, G.W. Trucks, H.B. Schlegel, G.E. Scuseria, M.A. Robb, J.R. Cheeseman, J.A. Montgomery, T.V. Jr., K.N. Kudin, J.C. Burant, J.M. Millam, S.S. Iyengar, J. Tomasi, V. Barone, B. Mennucci, M. Cossi, G. Scalmani, N. Rega, G.A. Petersson, H. Nakatsuji, M. Hada, M. Ehara, K. Toyota, R. Fukuda, J. Hasegawa, M. Ishida, T. Nakajima, Y. Honda, O. Kitao, H. Nakai, M. Klene, X. Li, J.E. Knox, H.P. Hratchian, J.B. Cross, C. Adamo, J. Jaramillo, R. Gomperts, R.E. Stratmann, O. Yazyev, A.J. Austin, R. Cammi, C. Pomelli, J.W. Ochterski, P.Y. Ayala, K. Morokuma, G.A. Voth, P. Salvador, J.J. Dannenberg, V.G. Zakrzewski, S. Dapprich, A.D. Daniels, M.C. Strain, O. Farkas, D.K. Malick, A.D. Rabuck, K. Raghavachari, J.B. Foresman, J.V. Ortiz, Q. Cui, A.G. Baboul, S. Clifford, J. Cioslowski, B.B. Stefanov, G. Liu, A. Liashenko, P. Piskorz, I. Komaromi, R.L. Martin, D.J. Fox, T. Keith, M.A. Al-Laham, C.Y. Peng, A. Nanayakkara, M. Challacombe, P.M.W. Gill, B. Johnson, W. Chen, M.W. Wong, C. Gonzalez, J.A. Pople, Gaussian 03, Gaussian Inc., Pittsburgh PA, 2003.
- [13] A.D. Becke, J. Chem. Phys. 98 (1993) 5648.
- [14] W.J. Hehre, R. Ditchfield, J.A. Pople, J. Chem. Phys. 56 (1972) 2257.
- [15] M. Dewar, W. Thiel, J. Am. Chem. Soc. 99 (1977) 4499.
- [16] M.J.S. Dewar, M.L. McKee, H.S. Rzepa, J. Am. Chem. Soc. 100 (1978) 3607.
- [17] C. Reichardt, Solvents and Solvent Effects in Organic Chemistry, WILEY-VCH, Weinheim, 2003.
- [18] D. Veierov, T. Bercovici, E. Fischer, Y. Mazur, A. Yogev, J. Am. Chem. Soc. 99 (1977) 2723.
- [19] Y. Sato, M. Morimoto, H. Segawa, T. Shimidzu, J. Phys. Chem. 99 (1995) 35.
- [20] N. Nagashima, S. Kudoh, M. Takayanagi, M. Nakata, J. Phys. Chem. A 105 (2001) 10832.
- [21] Y. Minoura, N. Nagashima, S. Kudoh, M. Nakata, J. Phys. Chem. A 108 (2004) 2353.
- [22] S. Coussan, Y. Ferro, A. Trivella, M. Rajzmann, P. Roubin, R. Wiczorek, C. Manca, P. Piecuch, K. Kowalski, M. Wloch, S.A. Kucharski, M. Musial, J. Phys. Chem. A 110 (2006) 3920.
- [23] H. Sterk, Monatsh. Chem. 100 (1969) 1246.
- [24] R.W. Bigelow, G.E. Johnson, J. Chem. Phys. 66 (1977) 4861.
- [25] W. Rettig, M. Zander, Chem. Phys. Lett. 87 (1982) 229.
- [26] L. Onsager, J. Am. Chem. Soc. 58 (1936) 1486.
- [27] W. Liptay, Excited States, Academic Press, New York, 1974.
- [28] A. Kapturkiewicz, J. Herbich, J. Karpiuk, J. Nowacki, J. Phys. Chem. A 101 (1997) 2332.
- [29] A. Kapturkiewicz, J. Herbich, J. Am. Chem. Soc. 120 (1998) 1014.
- [30] E.Z. Lippert, Naturforsch. 10a (1955) 514.
- [31] N. Mataga, Y. Kaifu, M. Koizumi, Bull. Chem. Soc. Jpn. 28 (1955) 690.
- [32] J. Karpiuk, J. Phys. Chem. A 108 (2004) 11183.
- [33] T. Soujanya, R.W. Fessenden, A. Samanta, J. Phys. Chem. 100 (1996) 3507.
- [34] K. Rechthaler, G. Kohler, Chem. Phys. 189 (1994) 99.
- [35] A. Samanta, J. Phys. Chem. A 105 (2001) 5438.